Safety classification of line lasers as extended source

Karl Schulmeister, Sarah Nagl, Reinhard Gilber

Journal of Laser Applications Vol. 38, paper 012007 (2026)
https://doi.org/10.2351/7.0001810

SAFETY CLASSIFICATION OF LINE LASERS AS EXTENDED SOURCE

Karl Schulmeister, Sarah Nagl, Reinhard Gilber

Seibersdorf Laboratories, Tech Campus, 2444 Seibersdorf, Austria

Abstract

Line lasers are good examples to discuss the safety classification of a laser product as extended source according to IEC 60825-1. It is necessary to consider different accommodations of the eye, from accommodation to the beam waist in the diverging axis (the vertex of the line) to accommodation to infinity, which results in a retinal line image. Measurements and the classification analyses were performed for a common line laser. It was found that accommodation to the beam waist in the diverging axis produces the most critical retinal image and can be considered as 'the apparent source'. Compared to the classification as a small source, classification as an extended source permits a factor of 5.8 higher power output. We argue that performing direct retinal image measurements with a CCD camera is more accurate and requires less effort than measuring beam parameters in the two axes and calculating the relevant parameters.

Introduction

Laser products are classified into laser safety classes according to IEC 60825-1 [1] and corresponding national implementations of this standard. For emission in the wavelength range between 400 nm and 1400 nm, the accessible emission limits (AEL) for Class 1, Class 2 or Class 3R are related to potential retinal injury. Line lasers are a classic type of laser product representing an extended source, associated to an extended retinal image. Compared to small sources that are associated to a minimum retinal image diameter, for a given laser class, extended sources are associated to higher permitted emission levels, which for line lasers has the advantage that the projected line appears 'brighter'. This type of laser product is called line laser because the emitted beam, at some distance from the laser product, is shaped like a line, as is shown in Figures 1 and 2. Using more scientific terminology, line lasers emit an extremely astigmatic beam, where one beam axis is very well collimated (here referred to as y-axis) while the other beam axis (x-axis) features a very high divergence. Such a beam geometry can be created when a well-collimated circular laser beam is incident on a cylindrical lens that is schematically shown in Figure 2 and can also be seen in the photograph (Figure 3).

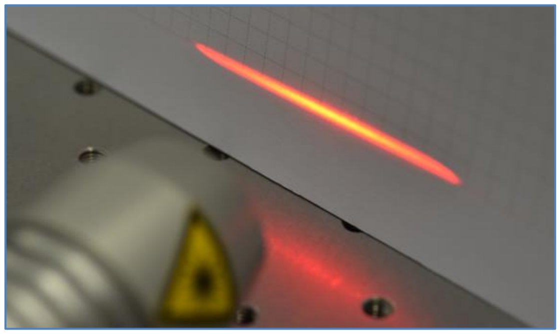

Figure 1. Photograph of the line-shaped laser beam incident on a piece of paper.

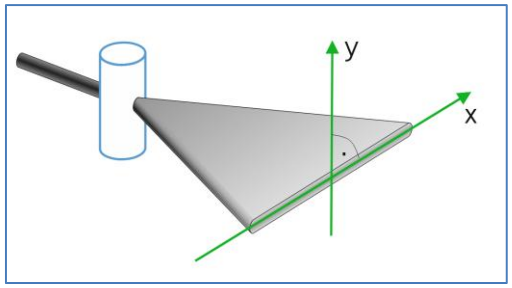

Figure 2. Schematic of a line laser beam formed when a well collimated circular laser beam passes through a cylindrical lens.

The cylindrical lens leaves the y-axis unaffected, i.e. well collimated, while for the x-axis, a beam waist is created in close proximity to the cylindrical lens, with a subsequently very high divergence in the x-axis. This beam waist is the vertex of the line from which the line 'fans out'.

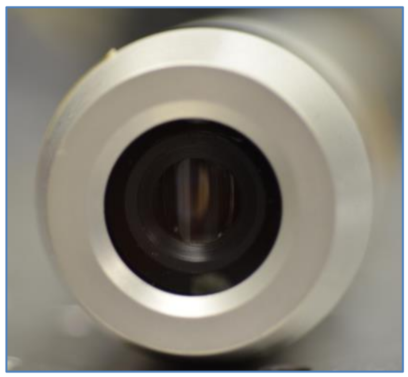

Figure 3. Photograph of the cylindrical lens of the line laser that was characterized.

Journal of Laser Applications
LIA THE LASER INSTITUTE

The principles of line lasers representing an extended source were already discussed by Henderson and Schulmeister [2]. Here, measurements that characterize the retinal image are presented for a specific product, demonstrating the importance of considering different accommodation positions of the eye, as required by IEC 60825-1:2014.

This paper was prompted by a recently published paper by Marshall et al. [3] on the classification of a line laser based on the measurement of the beam waist extent and the beam divergence in the vertical and the horizontal axis, and subsequent calculation of the parameters that are relevant for laser safety classification, particularly the extent of the retinal image and thus the angular subtense of the apparent source. We argue that it is more accurate and probably also less effort to determine the angular subtense of the apparent source directly via imaging onto a CCD camera. We will also show that hotspots in the retinal irradiance profile can be relevant, which cannot be characterized by a beam propagation method, which is only applicable for high-quality Gaussian beam profiles.

In the following, when the text refers to 'the IEC standard', IEC 60825-1:2014 is meant.

Methods

The laser under investigation emits laser radiation with a wavelength of 637 nm. For this wavelength, for Class 1, only the thermal retinal limit is relevant. The laser emits continuously, i.e. is not pulsed. If the emission were pulsed, the method would be equivalent to that as described, with the difference that the maximum field of view is limited to α_{max}, which can be as small as 5 mrad. Although not directly relevant for laser classification, the total beam power was determined as a reference value and was equal to 5.6 mW .

Only measurement Condition 3 (see Table 10 of the IEC standard) is analyzed. Condition 1 is not relevant, due to the highly divergent beam in the *x*-axis. For Condition 3, the radiant power of the laser beam passing through a 7 mm aperture stop was measured with a radiometer, having an integrated sphere fitted for optimum constant responsivity across the 7 mm aperture stop (transient recorder TR9600, Gigahertz Optik, Germany, expanded uncertainty equal to 1.7 % with coverage factor equal to 2). Classification as an extended source (subclause 5.4.3 of the IEC standard) for Condition 3 requires an assessment at 100 mm distance from the reference point of the product, as well as distances larger than 100 mm. For line lasers, according to Table 11 of the IEC standard, the reference point is the vertex of the beam in the diverging axis, i.e. the location of the beam waist in the *x*-axis.

The power as well as the CCD camera measurements were performed in the center of line, at the maximum of the beam's irradiance. It has to be noted that, depending on the type of line - shaping optics, the maximum of the power passing through the 7 mm aperture stop at 100 mm radial distance from the reference point may be found at the edges of the line rather than at the center. For the general case it is therefore necessary to vary the location of the analysis across the line profile.

The retinal irradiance profile was characterized by measurements with the CCD camera Ophir Optronics Solutions SP932U. An 'artificial eye' was assembled by placing the CCD camera in the image plane of a biconvex lens with 35 mm focal length. A 7 mm circular aperture stop was placed at the surface of the lens. The image distance was adjusted with a computer-controlled and calibrated linear stage and was varied in order to achieve different accommodation distances. When the CCD camera chip is in the focal plane of the lens, the optical location of the source that is imaged is at infinity, i.e. the artificial eye accommodates to infinity. To accommodate to closer distances, the CCD camera is moved to greater distances from the lens. IEC 60825-1:2014 implies that accommodation distances as close as 100 mm in front of the eye shall be considered for the analysis as extended source. It is important to analyze the CCD images in terms of angular subtense: distances on the CCD image in millimeter have to be converted into angular subtense by division by the image distance, i.e. the distance from the CCD chip to the principal plane of the lens. This is necessary in order to relate the artificial eye measurements that are performed with a fixed focal length lens to quantities relevant for retinal safety, which are given as angular subtense subtended by the retinal image as well as power or energy within a certain solid angle of the image, that is commonly referred to as field of view (FOV). With pixel dimensions of 3.45 µm, the angular resolution of the CCD image equals 0.10 mrad for accommodation to infinity and 0.065 mrad for accommodation 100 mm in front of the artificial eye. The symbol chosen by IEC 60825-1:2014 for the one-dimensional extent of the FOV (such as the diameter for a circular FOV) is γ, and the term used is acceptance angle. For a rectangular FOV, as is usually used for an analysis of limits related to the thermal retinal hazard, the angular width and height is here given the symbols γ_x and γ_y, respectively. For classification, the power (or energy) that is compared with the AEL is referred to as accessible emission, AE. For the analysis of extended sources, it is important to recognize that only the power that is within a given FOV needs to be compared with the AEL. In case the retinal image is larger than the FOV, the AE is smaller than the power that passes through the 7 mm aperture stop. For the analysis as small source, the value of the AE is equal to the power (or energy) that passes through the 7 mm aperture stop. IEC 60825-1:2014 subclause 4.3 d) for 'Non-uniform, non-circular or multiple apparent sources' specifies the method to analyze extended sources as relevant for the retinal thermal hazard, i.e. where the AEL features the parameter C_6. This image analysis method is described in more detail in our publications [4 - 6] and it is based on varying the extent and location of a rectangular FOV. Put into simple terms, the IEC standard requires to find that FOV which is associated to the maximum ratio of AE/AEL (see also the interpretation sheet ISH1 [7]). For the ratio, AE is the power (or for pulsed emission, the energy; in the following we refer to power only) within the respective FOV; the analysis can be performed in terms of fraction p as the ratio of the power within the FOV to the total power in the image (the power passing through the 7 mm aperture stop). In case the FOV is sufficiently large to encompass the whole image, $p = 1$. The determination of the AEL(α) is based on setting $\alpha_x = \gamma_x$ and $\alpha_y = \gamma_y$. The solution of the image analysis (the FOV with the maximum AE/AEL) provides two values: the value of α for the determination of the AEL and the power fraction p. The power passing through the 7 mm aperture stop, as measured with a power meter, represents the total power in the retinal image. Multiplication by p yields the AE as partial power of the image within the FOV.

Note 3 of subclause 4.3 d) of the IEC standard states that for Gaussian retinal image profiles, the d_{63} diameter can be used to determine the angular subtense of the apparent source, implying that in this case, AE is equal to the power that passes through the 7 mm aperture stop, i.e. the total power of the Gaussian retinal irradiance profile. Therefore, for non-Gaussian profiles, the method of varying the FOV described above must be used.

Results and Discussion

Before discussing the CCD camera measurements, we discuss the extended nature of line lasers on a phenomenological level. Let us assume that in each axis, the line shaped beam has a high beam quality (see also discussion by Marshall et al. [3]). For the y-axis this means that the beam is very well collimated, i.e. has a very small divergence. For the x-axis, focusing by the cylindrical lens produces a beam waist very close to the cylindrical lens. For the diverging line, this can be seen as vertex and is also referred to that way in Table 11 of the IEC standard. The width of this beam waist, for a high-quality beam in this axis, is very small. For an eye located 100 mm in front of the beam waist, accommodating to the beam waist (Figure 4a) produces a retinal image with minimum (1.5 mrad) angular subtense in the x-axis. For the standardized air-filled human eye, the distance between the rear nodal point of lens system and retina is 17 mm, so that a focal length of f = 14.5 mm results in accommodation to 100 mm in front of the eye. The highly collimated y-axis is associated to an 'apparent source' at infinity, as for any highly collimated beam. This means that accommodation to infinity (focal length of the eye of 17 mm) results in a minimum retinal y-axis extent, as shown in Figure 4b.

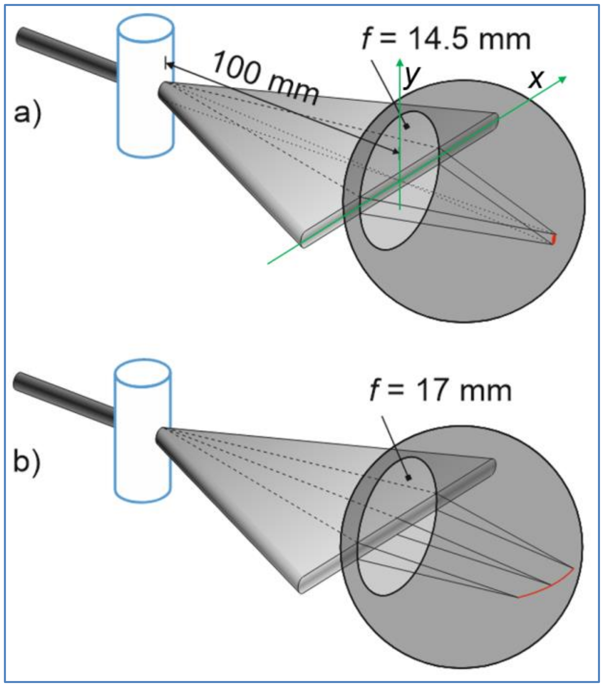

Figure 4. Schematic of a line laser and retinal images formed for accommodation to the line vertex assumed 100 mm in front of the eye (top), and to infinity (bottom).

Since in this qualitative discussion, the beam is assumed to be of high quality in both axis, there is an accommodation location that for each axis produces a minimum, i.e. small retinal image in that axis. For the well-collimated axis this is accommodation to infinity and for the highly diverging axis, this is accommodation to the line vertex, i.e. the beam waist in the x-axis. A line laser is an extended source, because for the respective other axis, the retinal image is extended, and it is apparent that the eye cannot accommodate to the two axis-worst-case locations at the same time. For accommodation to the vertex, the angular extent of the image in y-axis is equal to the angular extent the width of the beam at the respective location, i.e. basically the thickness of the line. For accommodation to infinity, if the 7 mm aperture stop would not intercept the beam, the retinal image extent in the y-axis would be equal to the divergence of the line-shaped beam. However, at a distance of 100 mm and further, the length of the line for common line lasers is always larger than 7 mm and consequently, the angular subtense of the retinal image in the *x*-axis is equal to 7 mm divided by the distance to the vertex.

The following data were obtained at a distance of 100 mm from the vertex of the line at the center of the line-shaped beam. The power passing through the 7 mm aperture stop was equal to 0.57 mW.

Figure 5 shows the CCD image for the accommodation that produced the maximum AE/AEL ratio, consistent with accommodation to the vertex, i.e. accommodation to the beam waist in the *x*-axis, from a reference distance of 100 mm.

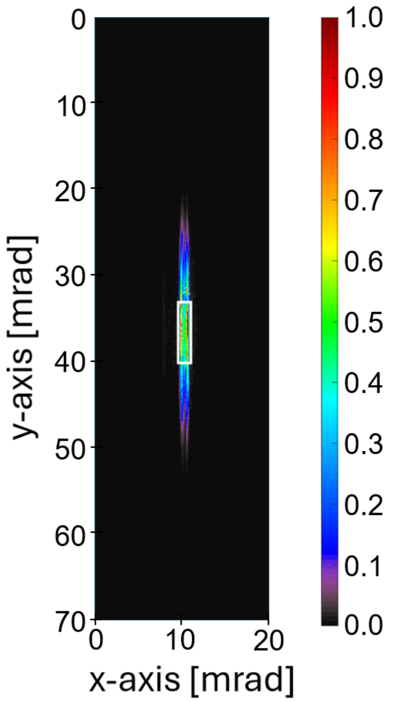

Figure 5. CCD image for the accommodation that produced the maximum AE/AEL ratio and is consistent with accommodation to the location of the beam waist in the *x*-axis, for a reference distance of 100 mm.

Since in this case, the 7 mm aperture stop does not influence the shape of the image, the irradiance distribution in the CCD image is a scaled representation of the irradiance profile that is located at the position of accommodation, which for Figure 5 happens to be at the position of the *x*-axis beam waist. Sometimes the terminology is also that this is the image of the apparent source, if the *x*-axis beam waist is considered as the apparent source. For this accommodation condition, the image analysis to determine the worst-case FOV (shown as white rectangle in Figure 5), for Class 1 and Class 2 has the same results. For the product measured, the beam waist diameter, and therefore the image extent in the *x*-axis is so small that it is assigned the minimum angular subtense of α_x = 1.5 mrad, which is the horizontal extent of the white rectangle shown in Figure 5. The vertical extent (*y*-axis) of the retinal image is related to the width of the beam in the *y*-axis (i.e. the thickness of the line) at the location of the *x*-axis beam waist. The image analysis yielded a critical FOV (see white rectangle in Figure 5) with $\gamma_y = \alpha_y$ = 7.1 mrad. We note that the vertical dimension of the critical FOV is smaller than the image profile, resulting in p = 0.49 and the AE = 0.28 mW being correspondingly smaller than the power passing through the 7 mm aperture stop (0.57 mW). We emphasize that it is only this fractional power, or partial power, that is used as accessible emission for the comparison with the AEL.

The above values of α_x and α_y obtained for accommodation to the vertex result in an averaged value of α = 4.3 mrad. The Class 1 AEL = 1.1 mW and the Class 2 AEL = 2.85 (see also values in Table 1). The AE/AEL ratio for Class 1 equals 0.25 and for Class 2 equals 0.10.

Table 1. Summary of classification analysis data.

	Class 1		Class 2	
Accomm.	infinity	vertex	infinity	vertex
α_x [mrad]	68.3	1.5	14.7	1.5
α_y [mrad]	1.9	7.1	1.5	7.1
α [mrad]	35.1	4.3	8.1	4.3
C_6	23.4	2.8	5.4	2.8
T_2 [s]	21.9	10.7		
AEL [mW]	7.57	1.10	5.39	2.85
p	0.96	0.49	0.24	0.49
AE [mW]	0.54	0.28	0.14	0.28
AE/AEL	0.07	0.25	0.03	0.10
Small source assumption				
AE [mW]	0.57	0.57	0.57	0.57
AEL [mW]	0.39	0.39	1.0	1.0
AE/AEL	1.46	1.46	0.57	0.57
More restrictive	20.3	5.8	22.1	5.8

Figure 6 shows the CCD image for accommodation to infinity. For accommodation to infinity, the Class 1 image analysis (with $T_2(\alpha)$ as factor in the AEL) produces a different critical FOV as compared to the Class 2 analysis. The false colors for the CCD images are adjusted to result in a dark red for the maximum irradiance within the image, which is at a different level depending on the accommodation and image (i.e. the colors of Figure 6 do not represent the same irradiance levels as the equivalent colors in Figure 5).

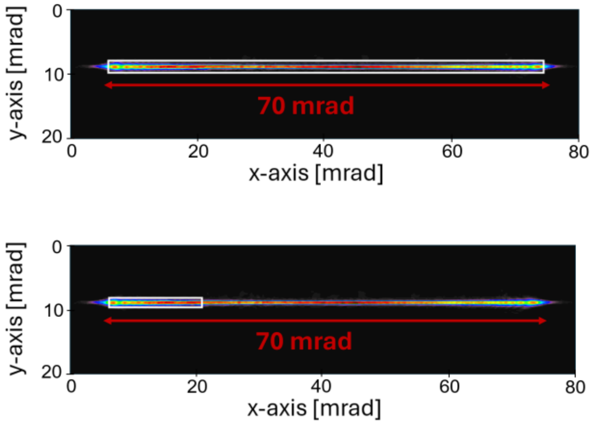

Figure 6. CCD image for accommodation to infinity. Top: image analysis for Class 1. Bottom: image analysis for Class 2. The color bar, normalized to 1, of Figure 5 also applies here.

We can see in Figure 6 that the *x*-axis extent, i.e. the length of the line, is limited to 70 mrad. This limitation is based on the rays that pass through the 7 mm aperture stop, as was discussed in our ILSC 2019 paper [5]. For a distance of 100 mm from the vertex , a 7 mm aperture stop results in an angular 'length' of the line equal to 7 mm/0.1 m = 70 mrad. The 'thickness' of the line image is small and the image analysis results in α_y = 1.9 mrad for the Class 1 image analysis and α_y = 1.5 mrad for the Class 2 image analysis. The rationale behind of the value of α_y = 1.9 mrad being marginally larger than 1.5 mrad can be understood considering that in the *x*-axis the image analysis resulted in a value close to 70 mrad. Thus, an increase of $\gamma_y = \alpha_y$ has little impact on the value of the AEL, but increases the AE somewhat, to encompass small contributions of the irradiance profile outside of 1.5 mrad. This results in a somewhat higher AE/AEL as compared to $\gamma_y = \alpha_y$ = 1.5 mrad.

For the Class 2 image analysis we note that the image analysis resulted in a rectangle that contains only a part of the line image (associated to p = 0.24 as partial power factor), not the full 70 mrad extent. The image analysis yields this rectangle as the one with the maximum AE/AEL ratio, because the retinal image features some irradiance irregularities at the end parts of the line. This produces a somewhat larger AE/AEL ratio as compared to the image analysis for Class 1 where the critical FOV has an extent of α_y = 68.3 mrad, i.e. almost 70 mrad and p = 0.96, i.e. almost equal to 1. The difference between the relative dependence on α is that for Class 1, not only C_6 depends on α but so does T_2. For Class 1 this favors the longer FOV over the shorter one. However, the difference in terms of AE/AEL ratio is very small: if one would use the critical FOV that was obtained for Class 1 for the Class 2 classification and not the rectangle as shown in the bottom part of Figure 6, the AE/AEL ratio would be only a factor of 11 % less restrictive.

For accommodation to infinity, the AE/AEL ratios are significantly smaller than the AE/AEL ratios for accommodation to the vertex. In other words, for the line laser under discussion, accommodation to the vertex is the more restrictive scenario for a distance of 100 mm from the vertex, and determines the class of the product. For the example measured, the product is Class 1.

For a given product distance, the location of accommodation that produces the most restrictive image and therefore the most restrictive AE/AEL ratio can be defined as 'the apparent source'. For the example of the line laser as measured, the vertex is the 'apparent source'. This is an example where looking into the laser beam (with filters for comfortable brightness levels) to qualitatively determine the 'apparent source' can be misleading. When looking into the beam at close distance to the cylindrical lens, the eye would naturally accommodate to infinity to produce a sharp line, much like the photo depicted in Figure 7 obtained with a photo camera focused to infinity. Thus, the source as it *appears* for a human is not the 'apparent source' as the quantitative result of a measurement according to the rules of IEC 60825-1:2014. It was already argued in [8] that each of the three words in 'The apparent source' can be seen as a misnomer, and line lasers are good examples to discuss the analysis method required for extended source laser products.

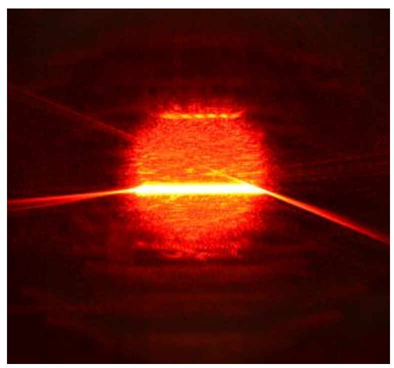

Figure 7. Photograph for accommodation to infinity, taken at a short distance from the cylindrical lens. While this is also the naturally obtained image for humans, it is not the worst-case retinal image and therefore not the image of the 'apparent source' following the rules of IEC 60825-1:2014.

That accommodation to the vertex produces the more restrictive retinal image is evident considering the much smaller retinal image, compared to accommodation to infinity. This is the result typical for common line lasers, provided that the line is not too 'thick' and that the product, for the vertex, does not feature some sort of distributed beam waist pattern or multiple lines, that for accommodation to the line - shaping optics would produce a relatively large retinal image. In special cases, if the retinal image for accommodation to the line - shaping optics is sufficiently large, accommodation to infinity can be associated to the more restrictive AE/AEL ratio and thus represent 'the apparent source'.

Above discussion provided the values of α and p for the two extreme cases of accommodation to infinity and accommodation to about 100 mm in front of the eye, the location of the x-axis beam waist.

For a distance of 100 mm from the cylindrical lens, retinal images were obtained starting with the CCD camera in the focal plane of the 35 mm focal length lens (resulting in accommodation to infinity) and a step-wise increase of the image distance with a step-distance equal to 0.2 mm, up to an image distance of 53.8 mm to result in an accommodation 100 mm in front of the artificial eye.

Figure 8 shows retinal images for accommodation to various locations in front of the artificial eye. The white rectangles show the solutions of the Class 1 image analysis. Figure 8 also shows an insert plotting the AE, Class 1 AEL and AE/AEL ratio as function of accommodation distance in front of the eye.

The different retinal images can be understood as the artificial eye looking through the cylindrical lens, imaging the virtual beam behind the cylindrical lens. The optical source that is imaged is the virtual irradiance profile that is present at the respective accommodation location, for the virtual beam. This association of the retinal image with the virtual beam profile at the location of accommodation, together with the potential influence of the 7 mm aperture stop limiting the retinal image, was discussed in detail in our 2019 ILSC paper [5].

For the analysis as extended laser source, IEC 60825-1:2014 requires that not only a distance of 100 mm from the reference point is considered, but also further distances. For some extended-source products, it is possible that further distances result in a larger AE/AEL ratio, i.e. a more restrictive scenario, as compared to 100 mm distance (see the more detailed discussion and the example in our 2015 ILSC paper on extended sources [4]).

For the line laser at hand, it was found that a distance of 100 mm is associated to the maximum AE/AEL ratio. Further distances resulted in somewhat smaller AE/AEL ratios, although the decrease as function of increasing distance is not very pronounced. This shallow dependence of the AE/AEL ratio as function of increasing distance r is typical for line lasers, both for accommodation to infinity as well as for accommodation to the vertex. The $1/r$ dependence of the power passing through the 7 mm aperture for the AE is similar to the decrease of the AEL based on the decrease of the angular subtense of the image. For accommodation to the vertex, this results in an AE/AEL ratio for a distance of 204 mm being only a factor of 1.18 less restrictive than the ratio for 100 mm distance, although the power passing through the 7 mm aperture stop at 204 mm is a factor of 2.05 smaller than at 100 mm distance.

With respect to the laser classification analysis based on the measurement of beam properties and the subsequent calculation of parameters relevant for product classification, as presented by Marshall et al. [3], we would like to comment that it appears that the measurement of the retinal image with a CCD camera is more direct, more accurate and possibly also less effort. Besides the difference in effort and complexity, the significant limitation of a beam propagation method is that it is only applicable for the case of beam with high-quality TEM_{00} Gaussian profiles in the two dimensions. We can see from the retinal irradiance profiles shown in Figure 8 that none of the retinal images exhibit a Gaussian irradiance profile in both dimensions. Thus, the assumption of a Gaussian beam profile for the beam propagation analysis by Marshall et al. [3] is not valid. For an accurate analysis, imaging with an 'artificial eye' and a FOV variation-image analysis is necessary, as required by IEC 60825-1:2014. For non-Gaussian profiles there is no beam property criterion available that would permit accurate laser safety calculations based on beam propagation [9].

Finally, the results of the classification as extended source are compared to a simplified small source analysis, i.e. assuming the retinal image is a small source, resulting in $\alpha = \alpha_{min}$ ($C_6 = 1$) and the AE being equal to the power passing through the 7 mm aperture stop at a distance of 100 mm from the vertex. As shown in the last three lines of Table 1, the permitted emission is a factor of 5.8 smaller than for the extended source analysis, causing a notable difference in line irradiance should the goal be to achieve, for instance, Class 2.

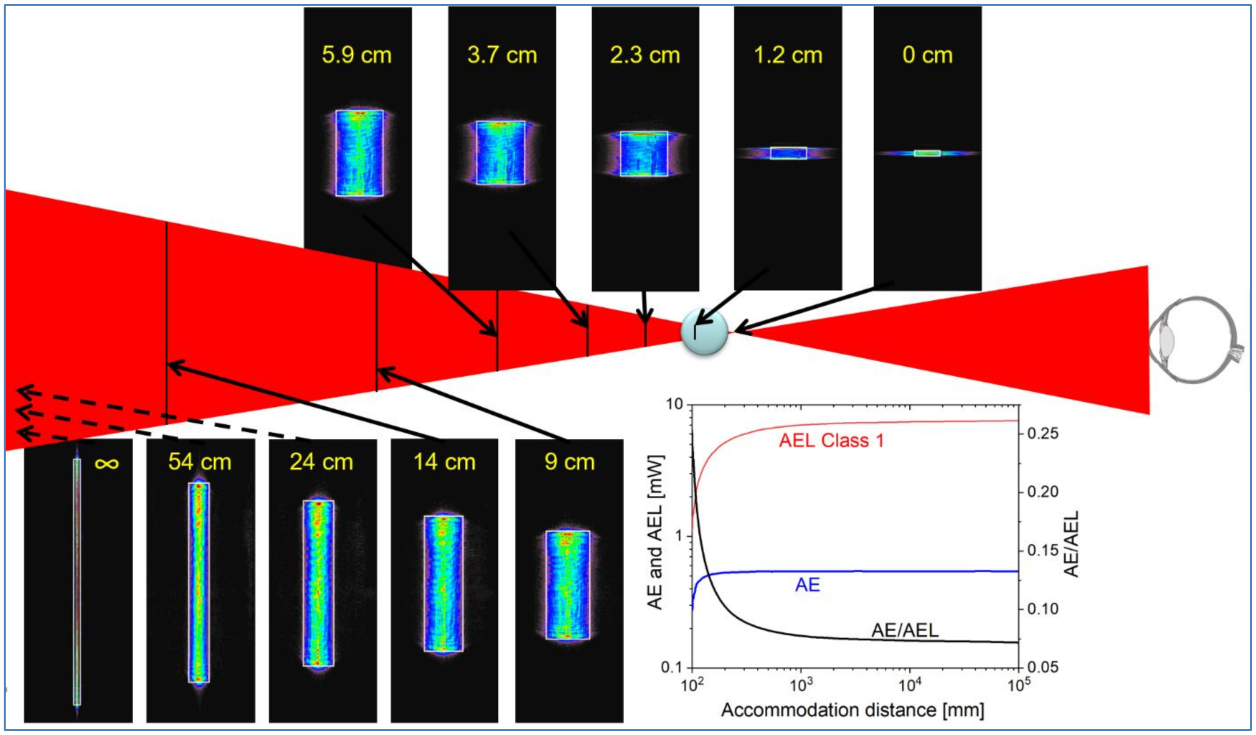

Figure 8. Assembly of CCD images for various accommodation locations, with the accommodation location measured in cm from the *x*-axis beam waist. The white rectangles are the solution of the image analysis based on Class 1 AELs. The insert shows classification-relevant parameters as function of accommodation distance relative to the location of the artificial eye, where accommodation to "infinity" (CCD chip in the focal plane of the lens) was plotted for 100 000 mm.

Summary and Conclusions

This study discusses the safety classification of line lasers as extended sources according to IEC 60825-1:2014. Line lasers are a good example of an extended source, since one of the two axes of the retinal image is always larger than α_{min}, i.e. extended. The retinal images can be understood as being associated with the irradiance profiles of the virtual laser beam when looking through the line - shaping optics, with due consideration of the potential effect of the 7 mm aperture stop limiting the extent of the retinal image in the diverging axis.

For a typical line laser, the most critical retinal image is produced when the eye accommodates to the beam waist in the highly divergent axis, i.e. accommodation to the vertex of the line. This condition defines the 'apparent source' for classification purposes, which is different to what a person perceives when looking into a line laser beam at close distance.

While the line laser in this study had a maximum irradiance in the center of the line, other types of line - shaping optics may produce higher irradiance levels at the edges of the line, which needs to be considered in a safety analysis.

We argue that, compared to measuring the beam parameters divergence and beam waist diameter in the two axes and calculating the parameters relevant for laser safety classification, directly measuring the retinal image using a CCD camera (with an artificial eye setup) provides a more accurate and less labor-intensive assessment of the angular subtense of the apparent source and of the AE within the critical field of view. Even a high - quality line laser beam may exhibit irregularities in its retinal image, so that it does not qualify as Gaussian profile. This necessitates the application of the image analysis method to the CCD image, as described in IEC 60825-1 for non-uniform retinal image profiles.

Classifying a line laser as an extended source, rather than a small source, allows for a significantly higher output power, in our example by a factor of 5.8, while maintaining a classification as 'safe' Class 1 or Class 2. This results in a brighter projected line, which is advantageous for practical applications.

References

[1] International Electrotechnical Commission (2014), IEC 60825-1 Safety of laser products – Part 1: Equipment classification and requirements, Ed 3.0, IEC, Geneva, 2014.

[2] Henderson R. and Schulmeister K. (2004), Laser Safety, Taylor & Francis Group, New York, London.

[3] Marshall W.J., Aldrich R.C., Frederiksen A. (2024), Laser hazard classification of a line laser with an astigmatic extended source, J. Laser. Appl. 36 022022. https://doi.org/10.2351/7.0001260

Erratum: https://doi.org/10.2351/7.0001741

[4] Schulmeister K. (2015), Classification of extended source products according to IEC 60825-1, ILSC 2015 Proceedings Paper C101, p. 271-280.

[5] Schulmeister K. (2019), Notes on the determination of the angular subtense of the apparent source in laser safety; ILSC 2019, Proceeding paper 1205, p. 284-293.

[6] Schulmeister K. (2024), Extended source AEL analysis of scanned laser emission for IEC 60825-1, White paper Seibersdorf Laboratories.

[7] IEC (2017), Interpretation Sheet 1 ISH1 for IEC 60825-1:2014.

[8] Schulmeister K. (2005), "The Apparent Source" – A Multiple Misnomer, ILSC 2005 Conference Proceedings, Laser Institute of America, p. 91-98.

[9] Schulmeister K., Gilber R., Edthofer F., Seiser B., Vees G. (2006), Comparison of different beam diameter definitions to characterize thermal damage of the eye, Proc. SPIE 6101 "Laser Beam Control and Applications", 61011A.

Meet the Authors

Karl Schulmeister, PhD, is a consultant for laser and lamp safety at Seibersdorf Laboratories in Austria. He has been actively involved in international standardisation of laser and lamp product safety for 30 years. Karl was the project leader for Edition 3 of IEC 60825-1 and has authored more than 100 papers. The injury threshold studies performed by his group formed the basis of the 2014 update of the IEC and ANSI exposure limits and AELs, including the *t*-dependent α_{max}. As consultant, he supports manufacturers with product safety analyses according to IEC 60825-1 as well as other photobiological safety standards.

Sarah Nagl, MSc, is a test engineer at the Test House for Laser and Lamp Safety of the Seibersdorf Laboratories in Austria. She focuses on the safety testing of products that emit laser and broadband radiation. In her master thesis, she specialized on the assessment of the potential photobiological occupational hazards of stage lighting using the Verordnung optische Strahlung, the Austrian implementation of the EU Artificial Optical Radiation Directive 2006/25/EC.

Reinhard Gilber, M.Eng., is a test engineer at the Seibersdorf Laboratories in Austria. He has specialized in the testing of complex laser products according to IEC 60825-1, including pulsed and extended sources, as well as scanned emissions resulting in time-varying retinal images. He also deals with the classification of broadband lamps according to IEC 62471:2006. As an electrical engineer he has specialized in the analysis of single fault conditions.